Modelling Tools for the Efficient Design of New Alloys

C J Humphreys and H K D H Bhadeshia
Department of Materials Science and Metallurgy
University of Cambridge
Pembroke Street, Cambridge, CB2 3QZ

1 ABSTRACT

Computer modelling techniques are a powerful new tool for the rapid design of new and improved materials. In this paper we describe three very different modelling methods and their applications. First, neural network modelling, which is ideal to predict the properties of complex systems, for example nickel-base superalloys, and to optimise their composition. Second, cluster variation method (CVM) modelling, which we apply to predicting which quaternary elements to add to a binary alloy, NiTi, with coherent ternary precipitates, Ni_2TiAl, in order to reduce the lattice misfit between the precipitates and the matrix. The CVM method also predicts the site occupancy of the quaternary elements and the phase they preferentially occupy. Third, density functional theory modelling to predict the nature of the atomic bonding in materials, which we apply to the intermetallic alloy series NiAl, CoAl and FeAl. We show that density functional theory predicts a covalent component to the bonding between the transition metal and Al, and that this will influence the dislocation mobility and hence the ductility in these materials.

2 INTRODUCTION

In the past, the development of a new aerospace material, from concept to application, has taken typically ten years. This paper will describe new computer-based modelling techniques which will optimise the development of new and improved alloys, greatly reduce the time-to-market and hence reduce the cost. Such modelling techniques will revolutionise the way gas turbine (and other) materials are developed.

A wide range of computer modelling techniques are being used and developed in Cambridge, in collaboration with others: ab initio quantum mechanical, neural network, kinetic, thermodynamic, finite element, etc. The models cover a range of length scales, from electronic to atomic to micro to macro levels. The models are being applied to the determination of phase stabilities, grain boundary structures, precipitation, segregation, grain size, flow stress, heat transfer, solidification, residual stress, creep, fatigue, lifetime, etc.

In this paper we will describe three different types of modelling:

(i) neural network modelling of γ/γ' nickel base superalloys.
(ii) Cluster variation method modelling of a potential new turbine disc material: $NiTi/Ni_2TiAl$.
(iii) Ab-initio calculations of the interatomic bonding in some aluminium intermetallics.

Simple binary intermetallics, such as NiAl, are materials which can in principle be modelled and understood using first principles calculations. However the nickel-base superalloys used for turbine blades typically contain 15 different elements, and with our present state of knowledge and computer power it is impossible to model these from first principles. Instead new neural network models have been developed in Cambridge to optimise such complex systems.

3 NEURAL NETWORK MODELLING OF Ni-BASE SUPERALLOYS

Despite decades of research on the γ/γ'nickel base superalloy system, new alloys have in the past been investigated by making as many as a hundred different variants. Each of these has to be cast or made into powder form, thermo-mechanically processed, assessed for the presence of deleterious phases and for processability, and tested on a laboratory scale. There is a further stage of optimisation before a small selection of alloys is tested to commercial standards. Predictive modelling, at any stage of this empirical alloy design procedure, would obviously reduce the cost and the time involved in the development of new materials.

Many mechanical properties are so complex in their dependence on material characteristics that there are no theories available to make quantitative predictions of the kind necessary in engineering design. The neural network method is ideal in such circumstances since it thrives in complexity, and when combined with experience from physical metallurgy, can be enormously useful both in the design of new materials and in the definition of critical experiments.

Neural networks are parameterized non-linear models used for empirical regression and classification modelling. Stated simply, this represents a method for the quantitative recognition of patterns in data, without any *a priori* specification of the nature of the relationship between the input and output variables.

They can model relationships of almost arbitrary complexity.

The outcome of neural network training is a set of coefficients (called weights) and a specification of the functions which in combination with the weights relate the input to the output. The training process involves a search for the optimum non-linear relationship between the inputs and the outputs and is computer intensive. Once the network is trained, estimation of the outputs for any given inputs is very rapid.

There are methods, such as that of MacKay[1], which implement a Bayesian framework on the neural network; this helps in the determination of the relevance of individual inputs. Furthermore, the error bars then depend on the specific position in input space, reducing the dangers of extrapolation and interpolation. These methods and associated references are described fully in MacKay et al[1]. We have found that the method is capable of revealing interesting metallurgical trends.

3.1 Overall Strength

The yield and ultimate tensile strength of nickel-base superalloys with γ/γ′ microstructures has been modelled[2,3] using the neural network method, as a function of the Ni, Cr, Co, Mo, W, Ta, Nb, Al, Ti, Fe, Mn, Si, C, B, and Zr concentrations, and of the test temperature. The analysis is based on data selected from the published literature. The trained models were subjected to a variety of metallurgical tests. As expected, the test temperature (in the range 25-1100 °C) was found to be the most significant variable influencing the tensile properties, both via the temperature dependence of strengthening mechanisms and due to variations in the γ′ fraction with temperature. Since precipitation hardening is a dominant strengthening mechanism, it was encouraging that the network recognised Ti, Al and Nb to be key factors controlling the strength. The physical significance of the neural network was apparent in all the interrogations we performed.

One example illustrating this last point is presented in Fig 1. The softening of the γ matrix is offset by the remarkable reversible increase in the strength of the γ′ with increasing temperature, the so-called anomalous yield strength effect which is observed in γ′. The neural network model correctly reproduces this behaviour.

A further revelation from the neural network analysis came from the error estimates, which demonstrated clearly that there are great uncertainties in the experimental data on the effect of large concentrations of molybdenum on the tensile properties. This has identified a region where careful experiments are needed; these will be conducted in future studies since molybdenum is known to have a large influence on the γ/γ′ lattice misfit.

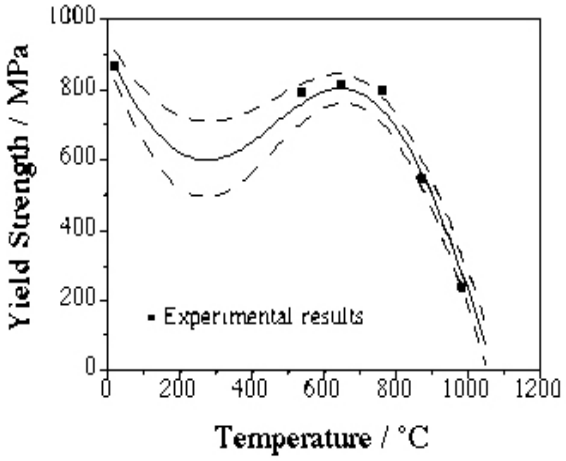

Fig 1: Predicted temperature dependence of the yield strength of a γ/γ′ superalloy.

The methodology for tensile properties has already been exploited in Rolls-Royce to reduce the number of variants involved in experimental alloy design programmes.

3.2 Fatigue Properties

An extensive literature review was carried out to assess methods for predicting fatigue crack growth rates. Physical models were examined but were either found not to be generally applicable or gave only qualitative indications of the trends[4]. Selected experiments were conducted[5] to clarify the factors controlling the initiation and propagation of cracks in turbine-disc superalloys. These results failed to clarify how fatigue theory could be used to make quantitative predictions.

A neural network method was therefore used after identifying some 51 variables that could be expected to influence the fatigue behaviour of nickel base superalloys[6]. The variables included stress intensity range ΔK, chemical composition, temperature, grain size, heat treatment, frequency, load, waveform, atmosphere, R-ratio, the distinction between short and long crack growth, sample thickness and yield strength. The analysis was conducted on some 1894 data collected from the published literature.

The model, unlike any experimental approach, could be used to study the effect of each variable in isolation. This gave interesting results. For example, it was verified that an increase in the grain size should lead to a decrease in the fatigue crack growth rate, when the grain size is varied without affecting any other input. This cannot be done in experiments because the change in grain size is achieved by altering the heat treatment, which in turn influences other features of the microstructure (Fig 2). It was also possible to confirm that log {ΔK} is more strongly linked to the fatigue crack growth rate than to ΔK, as expected from the Paris law. There are many other metallurgical trends

revealed[6]. The method has been used in the context of a Rolls-Royce disc alloy development programme, where it was demonstrated quantitatively that the uncertainties of current knowledge are so large that experiments were definitely necessary.

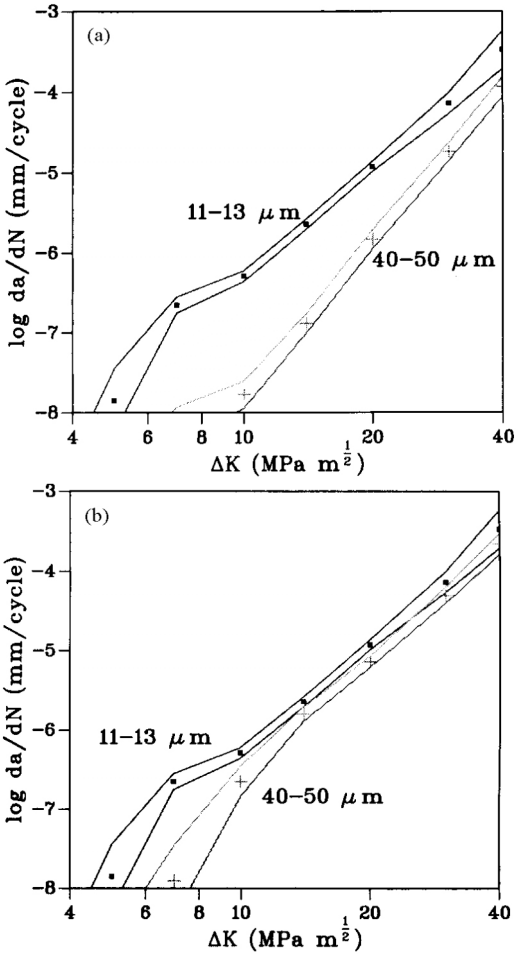

Fig 2: Astroloy: (a) effect of grain size alone; (b) effect of heat treatment alone[6].

In another approach[7] a different neural computing approach was used to focus on stage II of the Paris regime, where the growth rate should depend mainly on the stress intensity range, Young's modulus and yield strength. The model was used successfully in estimating new test data. The effect of the ultimate tensile strength and phase stability was also investigated; although this proved promising, it is probable that the results will be more convincing when a greater range of data become available.

3.3 Creep

The creep rupture life of nickel base superalloys has been modelled as a function of 42 variables including Cr, Co, C, Si, Mn, P, S, Mo, Cu, Ti, Al, B, N, Nb, Ta, Zr, Fe, W, V, Hf, Re, Mg, La and ThO_2[8]. Other variables include four heat treatment steps (characterised by temperature, duration and cooling rate), the sample shape and the solidification method.

The results have been interpreted using physical metallurgy principles where this is possible, and the model is currently being used in our Technology Foresight Programme.

3.4 Lattice Parameters

The lattice constants of the γ and γ′ phases of nickel superalloys have been modelled using a neural network within a Bayesian framework[9]. The analysis was based on new X-ray measurements and peak separation techniques, for a number of alloys and as a function of temperature. These data were supplemented using the published literature.

The lattice parameters of the two phases were expressed as a non-linear function of eighteen variables including the chemical composition and temperature. It was possible to estimate the uncertainties and the method has proved to be extremely useful in understanding both the effect of solutes on the lattice mismatch, and on how this mismatch changes with temperature. The method has been used in the development of new single-crystal alloys (TMS series) where rafting is an important phenomenon. The work will shortly be exploited in a theory for rafting, currently being developed in Cambridge.

3.5 Other Materials and Processes

The treatment of iron-base superalloys using both neural network and physical modelling is described in Badmos et al[10,11]; a description of the modelling of constitutive relations obtained by torsion testing is in Narayan et al[12]; the modelling of steel plate processing using more than 100 variables is in Singh et al[13].

4 DESIGNING A NEW LOW-DENSITY MEDIUM-TEMPERATURE ALLOY USING CLUSTER VARIATION METHOD MODELLING

We have attempted to design a new alloy for medium temperature applications, such as turbine discs operating at about 850°C. The materials currently used, nickel-base superalloys, have a density of about 8.3 g cm^{-3}. A number of intermetallics have much lower densities, for example NiAl (density 5.9 g cm^{-3}) or TiAl (density 3.8 g cm^{-3}) but they can be brittle at room temperature and much research has been performed in an attempt to increase their room temperature ductility. We have been pursuing a new approach: to start with an intermetallic, stoichiometric polycrystalline NiTi, which has relatively high room temperature ductility[14], and to attempt to increase its high temperature strength. NiTi has a density of about 6.5 g cm^{-3}, significantly lower than that of Ni-base superalloys, hence if it could be strengthened at 850°C whilst maintaining significant room temperature ductility it could be a candidate material to replace Ni-base superalloys in turbine discs.

4.1 $NiTi/Ni_2TiAl$ β/β′ Alloys

The specific yield stress (the yield stress divided by the density) of polycrystalline NiTi (which has the B2 CsCl

structure) is greatly increased at room temperature by the addition of Al at concentrations of more than 4 at %, which precipitates the Ni_2TiAl (β′) Heusler phase[14, 15, 16, 17]. For example, Ni_{50} Ti_{43} Al_7 has the β/β′ structure and exhibits a specific yield stress at room temperature of 250 MPa cm^3 g^{-1}. By comparison the specific yield stress at room temperature of NiTi and of Ni-base superalloys is 50 and 150 MPa cm^3 g^{-1} respectively. Thus at room temperature NiTi/Ni_2TiAl has a significantly higher specific strength than Ni-base superalloys.

However, as the temperature increases, the specific yield stress of NiTi/Ni_2TiAl falls until it equals the specific yield stress of Ni-base superalloys at about 600°C. At 800°C the specific yield stress of NiTi/Ni_2TiAl, for a 7 at % Al alloy, is only 60 MPa cm^3 g^{-1} compared with 130 for Ni-base superalloys. Electron microscopy reveals that the Ni_2TiAl precipitates grow at higher temperatures, for example after ageing at 800°C for 1000 hours the precipitates are typically at least 100 nm across and are incoherent, being surrounded by arrays of misfit dislocations.

The lattice misfit between β NiTi and β′ Ni_2TiAl is -1.43% at room temperature. One possibility is that the misfit strain energy provides the driving force for the precipitate growth, which is responsible for the alloy losing strength above 600°C. Hence if the lattice misfit can be reduced it may be possible to reduce the precipitate growth and hence to increase the high temperature strength of the alloy.

4.2 Misfit Control in Alloys using the Cluster Variation Method

The misfit between the Ni_2TiAl particles and the NiTi matrix can in principle be reduced by adding a quaternary element which partitions either in the Ni_2TiAl or in the NiTi in such a way as to reduce the misfit between them.

In our work[18] the cluster variation method (CVM) has been used to predict the partitioning of quaternary elemental additions between the β and β′ phases and the effect of these additions on the lattice misfit between the β′ precipitates and the β matrix. The predictions made by the CVM have been substantiated by X-ray diffraction misfit measurements and the resultant aged microstructures have been examined using transmission electron microscopy (TEM) techniques. The predicted phase partitioning behaviour of each dopant was confirmed through microanalytical techniques within a VG STEM.

The CVM has been successfully used to predict quaternary element partitioning and the effect on misfit in γ/γ′ Ni-based superalloys[15, 16]. Recently, Enomoto and Kumeta[17] have demonstrated the CVM as an effective tool in phase diagram prediction and misfit calculation in ternary β/β′ alloys. In our work, using the tetrahedron cluster approximation[18], the atomic arrangement and interatomic distances of Ni-Ti-Al-X alloys were optimised and thereby, the site occupancy. lattice misfit and equilibrium compositions of β and β′ phases were calculated simultaneously. To perform this calculation, the first and second nearest neighbour atoms were considered in the determination of cluster energy using Lennard-Jones phenomenological potentials. The potentials were determined from lattice parameter and thermodynamic data where available and by empirical predictions when not available.

Our CVM calculations predict that Ag, Co, Cr, Cu, Fe, Mo, Nb, Si, Ta, V and W will preferentially enter the β phase, except at temperatures lower than 900°C when Co and Cr will prefer the β′ and below 700°C when Fe and Cu will also prefer the β′ phase. In the β phase, the CVM model predicts Ag, Co, Cr, Fe, and Si will preferentially occupy the Ti site, and the other elements the Ni site. The CVM model further predicts that Fe and V should significantly decrease the lattice parameter of the β phase and hence reduce the misfit with the β′ phase. On the other hand, Ag is predicted to increase the misfit substantially. The other elements have little effect on the misfit.

In order to check these predictions, alloys were made up for selected dopant elements and X-ray diffraction measurements made of the lattice parameters and hence the misfits. High spatial resolution microanalysis was also performed. It was found that Cr, Nb and V do indeed partition to the β phase in a NiTi/Ni_2TiAl alloy. V and Fe reduce the lattice misfit between the phases, with Cr reducing it to a lesser extent. Co and Nb were found to have little effect on the lattice misfit, in agreement with the CVM model. Experimental ALCHEMI measurements showed that Cr preferred the Ti-sublattice in β, whereas Nb prefers the Ni-sublattice. Thus the CVM model correctly predicted the sense of both partitioning and misfit results, including the site preferences of Cr and Nb dopants.

The CVM model is a reasonably sophisticated model, and we tried two other models to see if they gave the same results. First, a size-factor (SF) strain model was used. This model is based on the concept that dopant atoms will preferentially partition to that phase for which the strain energy created by such doping will be minimised. In fact the size-factor model was not able to predict either the magnitude or even the sense of the effects of quaternary dopants on the β/β′ misfit. It is therefore clear that this simple model is inadequate.

We then used the MTDATA commercial model which enables phase diagrams to be caculated given thermodynamic data. Unfortunately, insufficient data are available for the NiTi/Ni_2TiAl system with quaternary additions. With the limited data available the MTDATA program correctly predicted the Cr partitioning behaviour, but was in error in the case of Nb.

We conclude that the CVM model is very useful for predicting the effects of quaternary dopants on the β/β′ misfit and also predicting the phase and site preference. The use of the CVM model can save a huge amount of experimental time.

5 UNDERSTANDING THE BONDING IN CRYSTALS USING DENSITY FUNCTIONAL THEORY

Why are many materials brittle at room temperature? Silicon is brittle because the covalent bonds between Si atoms make it difficult for dislocations to move. NaCl is brittle because the ionic bonds between Na^+ and Cl^- ions also make it difficult for dislocations to move. Copper, on the other hand, is ductile because the metallic bonding facilitates dislocation movement.

There are a number of factors which may be responsible for brittleness (for example, low dislocation mobility, lack of dislocation sources, grain boundary brittleness, etc), but in each case the nature of the bonding between atoms may be of fundamental importance. If we are to understand and control brittleness, it is important to understand the nature of the bonding in materials.

In recent years, density functional theory (DFT) has provided a framework which has greatly improved a range of band structure techniques (such as Linear Muffin Tin Orbitals (LMTO), pseudopotential methods, etc). In addition, the power of workstations has increased 100 times in the last six years, so that density functional theory calculations can now be performed on workstations.

Hence DFT can in principle be used to theoretically model the nature of the atomic bonding in, say, intermetallic materials. However there is a problem. Despite the huge theoretical advances in recent years, different theoretical methods using the DFT framework can still disagree significantly. For example, recently published calculated energies of a super-extrinsic stacking fault in TiAl are 110 mJm^{-2} using the LKKR method, but only 80 mJm^{-2} using the FLAPW method. The key question therefore is which calculation is correct, or are both wrong? Experiments are therefore essential to select the best theory. However once the best theory is selected for a particular material, then modelling using this theory can be extremely successful.

5.1 Density Functional Theory (DFT) and Electron Energy Loss Spectroscopy (EELS)

Recently a powerful new method has been developed to determine the bonding in materials based on a combination of experimental electron energy loss spectroscopy (EELS) and density functional theory (DFT)[19]. We will describe the use of this technique to the problem of determining the bonding in the intermetallics FeAl, CoAl and NiAl, which all have the same B2 crystal structure, but which have very different mechanical properties. Although density functional theory is required to interpret the EELS spectra in detail, many of the EELS results can be interpreted simply and quickly by inspection, as described later.

We have used the LMTO method with the local density approximation for exchange and correlation. The LMTO calculations were run self-consistently and EELS spectra were calculated by combining the computed density of states (DOS) with the matrix elements for the transition from initial to final states (see below). This treatment is based on the single-particle approximation of the EELS spectrum (see, for example, Botton and Humphreys[20]). We have also calculated spectra based on the more computationally demanding Korringa-Kohn-Rostoker (KKR) non-linear method for comparison (agreement is very good for the systems studied).

5.2 Electron Energy Loss Spectroscopy

In EELS, the fast incident electron excites electrons in the crystal from bound to unoccupied states (that is, states above the Fermi level). If the initial state has angular momentum L then the final states must have angular momentum L+1 or L-1. Hence if the initial state is a p state, the final state must be d or s. The EELS intensity for a transition from an initial state with angular momentum L to a final unoccupied state with angular momentum L+1 is:

$$I \propto |M_{L+1}|^2 \rho_L * \rho_{L+1} \qquad (1)$$

where ρ_L and ρ_{L+1} are the density of the initial states and the density of unoccupied final states, respectively, and * denotes convolution. For excitations from inner shells the density of initial states, ρ_L, is a delta function to a good approximation, hence

$$I \propto |M_{L+1}|^2 \rho_{L+1} \qquad (2)$$

Thus the intensity of EELS spectra is proportional to the density of unoccupied final states. This is an important result.

The matrix element M_{L+1} is given by

$$M_{L+1}=\int\psi_L^*(r)H\psi_{L+1}(r)dr \qquad (3)$$

where $\psi_L(r)$ and $\psi_{L+1}(r)$ are the initial and final state wavefunctions and H represents the electron-electron interaction. For non-zero M_{L+1} then ψ_L and ψ_{L+1} must overlap, hence if ψ_L is a localised core state, ψ_{L+1} must be local to the same atomic volume, hence EELS probes the local density of states.

For intermetallics based on transition metal elements (eg NiAl) we are particularly interested in the number of 3d electrons, hence in the transitions from initial 2p states to unoccupied 3d states. The 2p state is split into $2p^{3/2}$ and $2p^{1/2}$ initial states (spin-orbit coupled) hence the transition from 2p to 3d gives rise to two distinct sets of peaks, separated in energy (the $2p^{1/2}$ → 3d transition gives rise to the L_2 peak and the $2p^{3/2}$ → 3d transition to the lower energy L_3 peak). The L_2 and L_3 peaks are known as white lines since they appear on X-ray absorption spectra as white lines on a dark background.

5.3 Ni and NiAl: The Bonding Compared

Fig 3(a) shows experimental EELS spectra for the Ni L_{2-3} edges from fcc Ni and from NiAl. It is immediately apparent that EELS is sensitive to the bonding changes which occur when Ni goes from metallic Ni to NiAl. Fig 3(b) shows the LMTO calculated spectra, which agree well with the experimental spectra (except at higher energies about 10eV above the L_2 edge where the LMTO method does not consider enough basis functions). The more computer intensive KKR calculations are valid at higher energies and they not only agree with the experimental results and with the LMTO calculations to about 10eV above the L_2 edge, they also accurately reproduce the experimental intensity up to 50eV above the L_2 edge[20].

The Hume-Rothery rule for the valency of Ni when it is an "electron compound", as in NiAl, is that Ni has a full 3d band of ten electrons and an empty 4s band, so that its valency is zero. We can see from fig 3(a) that this is a simplistic way of considering the bonding in these materials. If Ni in NiAl had a full d band then there would be no L_{2-3} white lines. Hence from fig 3 there are unoccupied Ni d states in NiAl.

We can also see from fig 3(a) that the intensity of the Ni L_2 and L_3 white lines is stronger in metallic Ni than in NiAl. Since the EELS intensity is proportional to the density of unoccupied states it follows that there are more unoccupied Ni 3d states in metallic Ni than in NiAl at the Fermi energy. This effect is due to the fact that Ni 3d electrons hybridize with Al electrons when Ni is alloyed to become NiAl. Such an effect is confirmed by the analysis of the Al L_{2-3} edge which shows that Al s states hybridize with the Ni d bands and this results in the loss of "free metallic" character near the Fermi energy. At the same time, the experimental spectra and the calculations of the Al L_{2-3} edge show that there are common states between the Al and Ni atoms and this suggests that there is covalency in the bonds of NiAl[19].

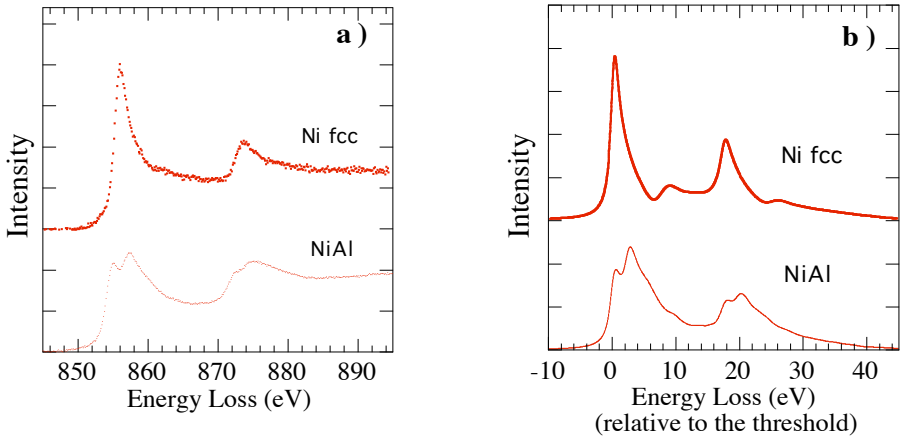

Fig. 3: Ni L_{2-3} edges in NiAl and fcc Ni. Experimental EELS spectra (a) and theoretical calculations using the LMTO technique (b).

5.4 NiAl, CoAl and FeAl: The Bonding Compared

The transition metal (TM) aluminides NiAl, CoAl and FeAl have the same crystal structure (B2) but very different mechanical properties. It is therefore of interest to see if EELS can detect changes in bonding in this series of neighbouring element TM aluminides. Since these materials have the same crystal structure they constitute an ideal test case to study systematic changes in the electronic structure which can potentially be related to changes in the mechanical or magnetic properties.

Fig 4 shows the experimental EELS L_2 and L_3 edges for Fe in FeAl, Co in CoAl and Ni in NiAl. The spectra have been recorded from regions of the same specimen thickness relative to the total inelastic mean free path so that any multiple inelastic scattering effects are comparable in the materials. Again, density functional theory LMTO calculations match well these experimental spectra[19] particularly for CoAl and NiAl. It is evident from fig 4 that the intensity of the Co L_{2-3} lines is greater than that of the Ni L_{2-3} lines. Since the intensity of these EELS spectra is proportional to the density of unoccupied 3d states we can immediately deduce that the transition metal d band fills on going from CoAl to NiAl. For FeAl, the single particle calculations using equation 1 and shown in fig 4(b) suggest a similar trend, that the transition metal d band fills on going from FeAl to CoAl. In the experiments, however, it is clear that this ground state effect is masked in part by the fact that excitation effects start to become more important for FeAl. This is shown by the fact that the agreement between theory and experiment is not as good as in NiAl (e.g. the position of the shoulder to the white-line moves to lower energy instead of higher energy) and there is also a broadening of the white-line relative to the Co L_{2-3} edge. Preliminary calculations accounting for some excitation effects (in particular a core-hole) show that the intensity at the threshold is lower than expected from a simple extrapolation of the trend observed on going from NiAl to CoAl. Hence the Fermi energy increases on going from FeAl to CoAl to NiAl. In fact the Ni d band in NiAl is nearly full so Hume-Rothery was nearly right!

It is clear from figs 3 and 4 that the TM L_2 and L_3 peaks of CoAl and NiAl (and to a lesser extent FeAl) are each split into sub peaks, whereas the L_2 and L_3 peaks from metallic Ni are not split. This can be explained from a consideration of the calculated density of states for the TM d band of the TM aluminides, which is a complicated function of energy with a number of oscillations[15]. The 3d density of states for the transition metals Ni, Co and Fe in the TM aluminides are broadly similar, but the position of the Fermi energy moves significantly, increasing from FeAl through CoAl to NiAl. Since the intensity of the EELS L_{2-3} edges is proportional to the density of states above the Fermi energy, the split L_2 and L_3 peaks correspond to oscillations of the DOS above the Fermi energy. The reversal of the relative heights of the split peaks in CoAl and NiAl (fig 5.2) is because the Fermi energy shifts and in CoAl it is near a maximum of an oscillation in the DOS, hence the first peak is high, whereas in NiAl it is near a minimum, hence the first peak is low[19]. For these compounds this peak represents an e_g band and thus orbitals pointing towards Al.

We have already shown that in going from metallic Ni to NiAl, electrons in the Ni d band hybridize. Similarly, by comparing EELS spectra from FeAl with those from metallic Fe, and from CoAl with those from metallic Co it is clear that in each case the d bands of the transition metal are affected in the same way.

Where do these hybridizing electrons come from? Al K-edge EELS spectra from metallic Al, FeAl, CoAl and NiAl show a pre-peak near the K-edge for FeAl, CoAl and NiAl, but not for metallic Al. Calculations confirm that this pre-peak is due to transitions from Al s to unoccupied 2p states in FeAl, CoAl and NiAl and this peak occurs at the same energy (relative to E_F) where the first peak in the TM edges is present. This observation and the results at the Al L_{2-3} edges in these compounds therefore represent the introduction of a directional covalent component to the Al-TM bonds. Hence there is a covalent component to the bond between Ni and Al, Co and Al, and Fe and Al and, as the Fermi energy moves in the band where the Al-p and TM-d bonds occur, the details of the bonding characteristics in these materials will therefore vary systematically.

5.5 Non-Stoichiometric $Ni_x Al_{1-X}$

Fig 5 shows EELS spectra from non-stoichiometric NiAl. It is clear that on the Ni-rich side the L_{2-3} peak intensity continuously varies with composition and provides a fingerprint of the local composition to about 1% compositional accuracy, with a spatial resolution that of the electron probe size, less than 1 nm in a field emission gun instrument. On the Ni-deficit side, the Ni L_{2-3} intensity is constant, although the background at higher losses varies as shown in fig 5.

Why does the Ni L_{2-3} EELS spectrum from non-stoichiometric NiAl vary in this way? On the Ni-rich side, there is evidence that the additional Ni atoms replace Al atoms and sit on the Al sub-lattice. A simple starting point to interpret the variation in the spectra is the following. Since almost zero-valency Ni is replacing trivalent Al, the Fermi energy decreases within the band and this results in it moving up a peak in the Ni density of states curve[21]. The first split peak of both the L_3 and L_2 white lines therefore increases as shown in fig 5. A more detailed analysis is described elsewhere[22].

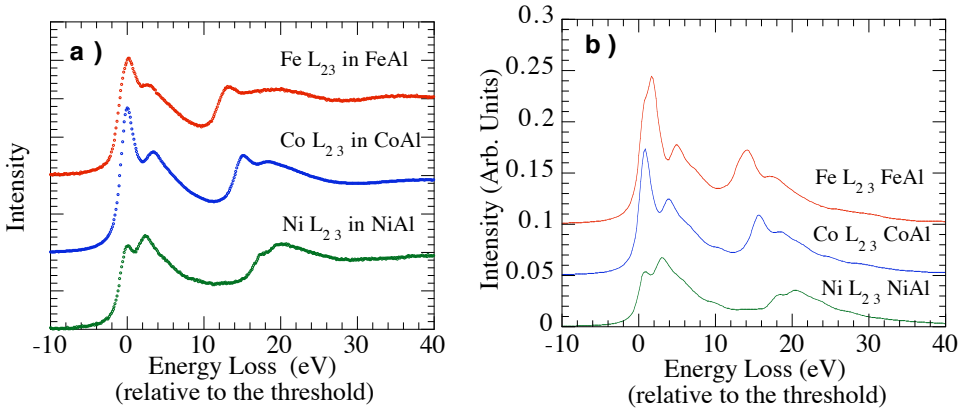

Fig 4: Transition metal $L_{2\text{-}3}$ edges in FeAl, CoAl and NiAl. Experimental edges obtained with EELS (a) and theoretical edges calculated with the LMTO method (b).

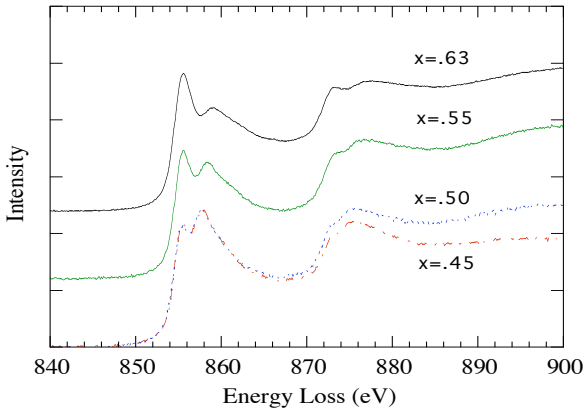

Fig 5: EELS Ni $L_{2\text{-}3}$ edges in non-stoichiometric $Ni_xAl_{1\text{-}x}$ as a function of composition.

In addition, we have calculated the Ni $L_{2\text{-}3}$ EELS spectrum for Ni atoms on the Al sub-lattice. The spectrum has a very strong first sub-peak and an almost absent second sub-peak for both the L_3 and L_2 white lines. By comparison, for Ni on Ni sites in NiAl, the first sub-peak is weaker than the second. Hence EELS can be used to determine site occupancies.

On the Ni-deficit side, Lipson and Taylor pointed out as long ago as 1939[23] that if Al has its usual valency of 3 and the valency of Ni is taken to be zero, then as Ni is removed from NiAl, leaving Ni vacancies, the average number of valence electrons per atom increases, and the number of atoms per unit cell decreases, but the number of valence electrons per unit cell remains constant (at 3). This is consistent with our observation of similar spectra in Ni-deficient alloys, and consistent with the conclusions of Cottrell[24] that there is no significant change in the bonding when constitutional vacancies are introduced in the Ni sub-lattice.

5.6 Phase Stability

A high density of states at the Fermi energy usually results in low phase stability because the total electron energy is high[25]. We can fix the position of E_F on the density of states curve from density functional theory and confirm this using EELS. For the alloys considered in this paper, the density of states at the Fermi energy is highest for FeAl and lowest for NiAl, with CoAl lying between.

Experimentally, all these alloys are ordered up to their melting point, but FeAl exhibits the highest degree of local disorder as is evident from diffraction patterns in which there is significant diffuse scattering from FeAl. The diffuse scattering is due to small atomic displacements, probably induced by thermal vacancies which have a particularly high density FeAl. Thus EELS can be used to study phase stability.

5.7 TiAl and The Single Particle Approximation

We have shown above the good agreement between theory and experiment for EELS spectra from NiAl and CoAl. The agreement is less good for FeAl and significantly less good for TiAl[20] due to the breakdown of the single particle approximation used in writing down the equations in section 5.2.

The problem arises for two main reasons:

(i) When an electron is excited from a 2p state to an empty 3d state it leaves behind a hole in the 2p state. This core hole interacts with the excited electron, but this interaction is neglected in the single particle approximation. The reason this approximation works well for EELS spectra from NiAl and CoAl is because they have many 3d electrons which screen the excited electron from the core hole. However, TiAl has fewer 3d electrons and hence the screening is less effective. This effect starts to be seen in FeAl as discussed above.

(ii) The single particle approximation neglects the d-d electron interaction between the excited electron and the other d band electrons (although the theory takes into account exchange and correlation effects between all electrons in the ground state wavefunction). In the late TM aluminides (NiAl and CoAl) there are a limited number of unoccupied states available to the excited electron, so exchange and correlation effects with this electron are small. However, in the early TM aluminides (for example, TiAl) due to the relatively empty 3d band exchange and correlation effects are large.

Hence for the quantitative interpretation of EELS spectra from early TM aluminides, the single particle approximation partially breaks down and a theory is required which fully takes into account not only the ground state but also the excited state and the excitation process, including all exchange and correlation effects and the core hole.

6 CONCLUSIONS

Modelling techniques are very powerful for understanding and predicting a wide range of physical phenomena. In particular they will enable us to design new and improved materials for gas turbines much more rapidly than the trial-and-error experimental methods that have been largely used in the past.

In this paper we have described three very different modelling techniques and their applications. First, neural network modelling. In recent years, neural networks have greatly improved and they are ideal for complex systems for which a large amount of experimental data already exists. A ‘trained’ neural network can then be used, for example, to optimise the composition of an alloy for a given property, for example strength, or for a given combination of properties. Neural networks have already been used to optimise Ni-base superalloys for turbine blades.

Second, we have shown how cluster variation method (CVM) modelling can be used to predict the phase into which a quaternary dopant element will partition, and the atomic sublattice on which it will sit. CVM modelling can also be used to predict the change in lattice parameter which occurs on doping and hence to predict how the lattice mismatch between a coherent precipitate and its matrix can be increased or decreased by doping with the appropriate element. CVM modelling greatly reduces the time which would be required to solve problems such as this experimentally.

Finally, we have shown how on a very basic level, density functional theory (DFT) can be used to understand and predict the atomic bonding in alloys, which is of fundamental importance in controlling dislocation mobility and hence ductility.

Mathematical modelling will undoubtedly become an increasingly important design tool for new and improved alloys tailored to specific applications. It should greatly reduce the time-to-market for new and improved materials.

7 REFERENCES

1. MacKay, D.J.C., "Bayesian non-linear modelling with neural networks", in Cerjak, H. and Bhadeshia, H.K.D.H. (eds), "Mathematical Modelling of Weld Phenomena III", London, UK, Institute of Materials, 1997, p359-389.

2. Jones, J. and MacKay, D.J.C., "Neural network modelling of the mechanical properties of nickel base superalloys", in "8th Int. Symposium on Superalloys", Seven Springs, Pennsylvania, USA, Kissinger, R.D. et al. (eds), published by TMS, 1996, pp 417-424.

3. Jones, J. Mackay, D.J.C. and Bhadeshia, H.K.D.H., "The strength of nickel-base superalloys: a Bayesian neural network analysis", in "Proc. 4th International Symposium on Advanced Materials", Anwar ul Haq et al. (eds), A. Q. Kahn Research Laboratories, Pakistan, 1995, pp 659-666.

4. Schooling, J.M., "The modelling of fatigue in nickel base alloys", PhD Thesis, University of Cambridge.

5. Schooling, J.M. and Reed, P.A.S., "The application of neural computing methods to the modelling of fatigue in nickel-base superalloys", in "8th Int. Symposium on Superalloys", Seven Springs, Pennsylvania, USA, Kissinger, R.D. et al. (eds), published by TMS, 1996, pp 409-419.

6. Fuji, H., Mackay, D.J.C. and Bhadeshia, H.K.D.H., "Bayesian neural network analysis of fatigue

crack growth rate in nickel-base superalloys", ISIJ International, Vol. 63, 1996, pp 1373-1382.

7. Schooling, J.M. and Reed, P.A.S., "The effect of load ratio on near-threshold fatigue crack propagation in a nickel-base superalloy", in "Proc, 4th International Symposium on Advanced Materials", Anwar ul Haq et al. (eds), A. Q. Kahn Research Laboratories, Pakistan, 1995, pp 555-561.

8. Fujii, H., Mackay, D.J.C., Bhadeshia, H.K.D.H., Harada, H. and Nogi, K., "Estimation of creep rupture strength in nickel-base superalloys", in press, "6th Leige Conference, Materials for Advanced Power Engineering", Leige, Belgium, 1998.

9. Yoshitake, S., Narayan, V., Harada, H., Bhadeshia, H.K.D.H. and Mackay, D.J.C., "Estimation of the γ and γ' lattice parameters in nickel-base superalloys using neural network analysis", ISIJ International, Vol.38, 1998, pp 495-502.

10. Badmos, A.Y., Bhadeshia, H.K.D.H. and Mackay, D.J.C., "Tensile properties of mechanically alloyed oxide dispersion strengthened iron alloys. Part 1 - Neural network models", Materials Science and Technology, Vol. 14, 1998, pp 793-809.

11. Badmos, A.Y. and Bhadeshia, H.K.D.H., "Yield strength of mechanically alloyed ODS iron alloys. Part 2: Physical interpretation", accepted for publication in Materials Science and Technology, 1997.

12. Narayan, V., Abad-Lera, R., Lopez, B., Bhadeshia, H.K.D.H. and MacKay, C.J.C., "Estimation of hot torsion stress-strain curves in iron alloys using a neural network analysis", submitted to ISIJ International, 1998.

13. Singh, S.B., Bhadeshia, H.K.D.H., Mackay, D.J.C., Carey, H. and Martin, I., "Neural network analysis of steel plate processing", accepted for publication in Ironmaking and Steelmaking, 1998.

14. Koizumi, Y., Ro Y., Nakazawa, S. and Harada, H., "Intermetallic alloys strengthened by Al substitution", in "Symposium on Atomic Arrangement Design and Control for New Materials", Tsukuba, Japan, 1994, p 36. Also in Mat. Sci. and Eng., A223, 1997, 36.

15. Oh-ishi, K., Tian, W.H., Sano, T. and Nemoto, M., "Phase decomposition and hardening in NiAl-NiTi pseudo-binary alloy system", J. Japan Inst. Metals, 60, 1996, pp 239-246.

16. Warren, P.J., Koizumi, Y., Murakami, H. and Harada, H., "Phase decomposition in NiTi-Ni_2TiAl alloy system", paper presented at the 3rd Int. Charles Parson's Turbine Conference, Newcastle, UK, 1995, p26.

17. Peters, M.A., Botton, G.A. and Humphreys, C.J., "The precipitation of β' Ni_2TiAl from Al-doped β Ni-Ti alloys", Inst. Phys. Conf. Ser., 147, 1995, pp 451-454.

18. Peters, M.A. and Humphreys, C.J., "Misfit control in NiTi/Ni_2TiAl alloys", in Nathal, M.V., Davolia, R., Liu, C.T., Martin, P.L., Miracle, D.B., Wagner, R. and Yamaguchi, M. (eds), Structural Internetallics 1997, The Minerals, Metals and Materials Society, 1997, pp 605-612.

19. Botton, G.A., Guo, G.Y., Temmerman, W.M. and Humphreys, C.J., "Experimental and theoretical study of the electronic structure of Fe, Co and Ni aluminides with the B2 structure", Phys. Rev. B., 54, 1996, pp 1682-1691.

20. Botton, G.A. and Humphreys, C.J., "Analysis of EELS and near edge structures to study the bonding character in intermetallic alloys", Micron, 28, 1997, pp 313-319.

21. Botton, G.A., Guo, G.Y. and Humphreys, C.J., "The bonding character of intermetallic alloys using EELS", Inst. Phys. Conf. Ser. No 147, EMAG 95, Birmingham, 1995, pp 535-538.

22. Botton, G.A., Guo, G.Y., Temmerman, W.M., Stozek, Z., Humphreys, C.J., Yang Wang, Stocks, G.M., Nicholson, D.M.C. and Shelton, W.A., in preparation, 1999.

23. Lipson, H and Taylor, A., Proc. Roy. Soc., A713, 1939, p 232.

24. Cottrell, A.H., "Constitutional Vacancies in NiAl", Intermetallics, 3, 1995, p 341-345.

25. Freeman, A.J., Hong, T., Lin, W., Xu, J-U., "Phase-stability and role of ternary additions on electronic and mechanical properties of aluminium intermetallics", in "High-temperature ordered intermetallic alloys IV", Johnson, L.A., Pope, D.P., Stiegler, J.O. (eds), Materials Research Society, Pittsburgh, 1991, 158, pp 3-18.